Top-down solar modulation of climate: evidence for centennial-scale change

2010 Environ. Res. Lett. 5 034008

(http://iopscience.iop.org/1748-9326/5/3/034008)

Environ. Res. Lett. **5** (2010) 034008 (9pp) doi:10.1088/1748-9326/5/3/034008

Top-down solar modulation of climate: evidence for centennial-scale change

M Lockwood[1,2], C Bell[1], T Woollings[1], R G Harrison[1], L J Gray[1] and J D Haigh[3]

[1] Space Environment Physics Group, Department of Meteorology, University of Reading, Earley Gate, PO Box 243, Reading RG6 6BB, UK
[2] Space Science and Technology Department, Rutherford Appleton Laboratory, Harwell Campus, Chilton, Didcot, Oxfordshire OX11 0QX, UK
[3] Space and Atmospheric Physics Group, Blackett Laboratory, Imperial College, London SW7 2AZ, UK

E-mail: m.lockwood@reading.ac.uk

Received 5 June 2010
Accepted for publication 10 August 2010
Published 20 August 2010
Online at stacks.iop.org/ERL/5/034008

Abstract
During the descent into the recent 'exceptionally' low solar minimum, observations have revealed a larger change in solar UV emissions than seen at the same phase of previous solar cycles. This is particularly true at wavelengths responsible for stratospheric ozone production and heating. This implies that 'top-down' solar modulation could be a larger factor in long-term tropospheric change than previously believed, many climate models allowing only for the 'bottom-up' effect of the less-variable visible and infrared solar emissions. We present evidence for long-term drift in solar UV irradiance, which is not found in its commonly used proxies. In addition, we find that both stratospheric and tropospheric winds and temperatures show stronger regional variations with those solar indices that do show long-term trends. A top-down climate effect that shows long-term drift (and may also be out of phase with the bottom-up solar forcing) would change the spatial response patterns and would mean that climate-chemistry models that have sufficient resolution in the stratosphere would become very important for making accurate regional/seasonal climate predictions. Our results also provide a potential explanation of persistent palaeoclimate results showing solar influence on regional or local climate indicators.

Keywords: solar variability, regional climate, solar UV emission, stratosphere–troposphere coupling

Dedicated to the memory of Dr Chris Bell (1983–2010)
Chris Bell was the main author of the atmospheric responses section of this paper. Tragically, shortly after it was submitted, he was hit by a car while walking home and never regained consciousness. As well as being a highly skilled, insightful and knowledgeable scientist, Chris had a delightful character with a sense of fun allied to an infectious enthusiasm. We miss him greatly.

1. Introduction

Several solar parameters and outputs during the recent sunspot minimum were lower than for the previous minima during the space age, indeed lower that at any time since about 1920 [1]. The decline in UV emission during the descent into this exceptional solar minimum was monitored by the SIM instrument on the SORCE satellite and revealed a larger change [2] than seen by different instruments at the corresponding phase of previous solar cycles [3, 4], particularly at the wavelengths responsible for stratospheric ozone production and heating [5] with consequences for

the patterns of winds and temperatures throughout the stratosphere [5, 6]. However, there is debate about the calibration of the recent data and hence whether UV irradiances in the recent solar minimum were really lower [7].

There is growing evidence that dynamical coupling across the tropopause means that stratospheric changes can influence the underlying troposphere [6, 8] and under some circumstances, robust tropospheric responses are indeed predicted by models. Tropospheric jet streams have been predicted to be sensitive to the solar forcing of the stratosphere [9, 10]. This could occur through disturbances to the stratospheric polar vortex [11] which are observed to propagate downwards to affect the tropospheric jets [12]. (However, it should be noted that the fact that the disturbances appear first in the stratosphere does not necessarily mean that the stratosphere is driving the troposphere [13].) Alternatively, solar-induced stratospheric changes may influence the refraction of tropospheric eddies [14, 15]. Models (e.g., [16]) do predict that perturbations can descend from the stratosphere to the surface by altering the propagation of planetary waves coming up from the surface, an effect that has been reported in observations [17]. Definitive identification of these 'top-down' solar influences on the troposphere is difficult; however, models show that the stratosphere has the potential to play a crucial role in regional climates. For example, Scaife *et al* [18] have demonstrated that stratospheric trends over recent decades, along with downward links to the surface, are indeed strong enough to explain much of the prominent trend in the North Atlantic Oscillation (NAO) between the 1960s and the 1990s, with implications for regional climate in Europe, particularly in winter. Effects have also been identified in the southern hemisphere [19].

These 'top-down' mechanisms would be effective alongside 'bottom-up' solar heating of the sea surface and the dynamically coupled air–sea interactions [20]. Although differentiating between the effects of variations in the two will often be difficult, recent studies indicate that they are additive, producing amplified SST, precipitation and cloud responses, for example in the tropical Pacific, even for relatively small solar forcing changes [21, 22]. The solar output driving the bottom-up effects is the total solar irradiance (TSI) whereas for top-down forcing the spectral solar irradiance in the UV band is relevant. This paper investigates UV spectral variability. The effects on climate of solar variations have been shown to be swamped by anthropogenic effects in recent decades on global scales (e.g., [23]), but they have also been found to be significant in certain regions and seasons [24–26]. Significant differences between mean global mean air surface temperature for composite surface temperature maps at low and high sunspot activity have been found [27]. Such a signal can also be seen in both the ECMWF ERA40 and NCEP/NCAR re-analysis datasets, in which observations have been assimilated with model data [28]. This signal is weaker in the ERA40 dataset and varies regionally [27, 29]. We here present evidence for long-term drift in UV irradiance, which is not found in its commonly used proxies, and that both stratospheric and tropospheric winds and temperatures show stronger regional responses to those solar indices that show long-term trends.

2. Solar UV irradiance

The 10.7 cm solar radio flux, $F10.7$, originates from about $h_S = 2100$ km above the visible solar surface at the large temperature gradient: this is associated with the strong emission of Lyman-α at 120 nm [30] which produces a temperature plateau that is eroded by ambipolar diffusion. The temporal variation of $F10.7$ is closely mirrored by the core-to-wing ratio indices of absorption lines, such as Ca-II (wavelength $\lambda \approx 393$ nm) and Mg-II (280 nm) where the wing emission, like the rest of the UV continuum, arises at $0 < h_S < 300$ km but the absorption determining the line core takes place at about $900 < h_S < 2000$ km. Thus the indices commonly used to quantify solar UV emission (Ly-α [30], Ca-II [31], Mg-II [32], and $F10.7$ [30]) are all determined by the upper chromosphere, whereas the continuum UV emission arises from below the minimum of the temperature profile, i.e. below $h_S \approx 400$ km for $\lambda > 160$ nm. The correlations between a given UV spectral band and these indices vary and depend on timescale [33]. Hence good agreement on one timescale does not preclude differences on another. Thus the fact that the commonly used proxies for solar UV emission reproduce the solar cycle and solar rotation variations in the UV emission rather well does not necessarily mean that they will also capture its centennial-scale drift. The large difference between the observed UV emission during recent solar minimum [2] and during previous minima [3, 4] can have one, or a combination, of three causes: (a) the new data are in error [7]; (b) the previous data were in error or (c) there has been a real change in the emission, associated with the recent exceptionally low solar minimum. We here investigate possibility (c): because we are concerned with the variation and not the absolute levels, (a) and (b) can be considered together by looking at the intercalibration of the new and the previous data.

We employ the UV spectral irradiance (S) composite (as a function of time t and wavelength λ) by DeLand and Cebula [4] and add the more recent SORCE data [2]. The composite was compiled using absolute calibration but at some λ this leads to discontinuities in the temporal sequences at the joins between the data from different sources. We here use monthly means for each λ (1 nm apart) and make zero-level adjustments at each join. To do this, we employ the high correlations (r_{SP}) on short (1 year) timescales between S and the Ca-II, Mg-II and $F10.7$ proxies. Figure 1 demonstrates the procedure for a particularly clear example. For every known change in the source of the data ('join'), monthly means of S (at the λ in question) were taken for one year before and after the join. The data for one year after the join (filled black circles) was compared to that for one year before it (filled grey squares). A least-squares linear regression between the S data after the join and the proxy ($F10.7$ in the example shown in figure 1) was generated and is shown by the solid line. The best-fit zero-level offset for the data from before the join, ΔS, was then derived such that, when corrected by ΔS (open triangles), the mean square deviation from the regression line is minimized. Note the correction is applied to all data before the join, so that all corrected data become relative to the most recent data. The offset used is the

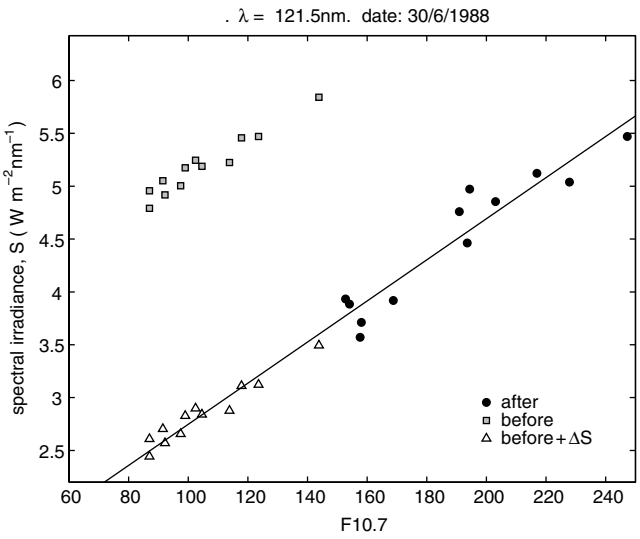

Figure 1. Illustration of the procedure used to intercalibrate data in the composite UV data series. This example is for a wavelength $\lambda = 121.5$ nm and uses the relationship to the $F10.7$ proxy on timescales of order 1 year. For every known join between different data sources (this one is on 30th June, 1988), the monthly means for one year before the join (grey filled squares) were compared to the monthly means for one year after the join (black filled circles). Only corrections for zero-level offsets are made and it is assumed that instrument gain factors are constant. The data from after the join were regressed against the proxy (solid line) and the data from before the join were corrected (giving the open triangles) by a constant offset ΔS which gives the best least-squares fit to the solid line.

best of those derived from the three proxies, as evaluated using the rms deviation from the regression line (for the data after the join plus those before it after correction: i.e., the solid points plus the open triangles in figure 1). Useable corrections were obtained everywhere except for before 1986 at $\lambda > 270$ nm: these data were discarded. No assumptions were made about the shape of the spectrum and so no corrections were applied in the λ dimension.

Figure 2(b) shows the minimum (in blue) and maximum (in red) of monthly means of S as a function of λ for the interval covered by the composite (1979–2010). Note that these spectra are given on a logarithmic S scale. It can be seen that the solar cycle variation is a very small fraction of the mean level, especially at the larger λ. Part (c) of figure 2 shows normalized variations of S by colour contouring $(S - \langle S \rangle)/\sigma_S$, where $\langle S \rangle$ and σ_S are the mean and standard deviation of S for the full interval and the λ in question, as a function of time t and wavelength λ. This plot reveals clear solar cycle signals (compare with $F10.7$ in figure 2(a)) at most λ. It can be seen that the calibration procedure yields some discontinuities in the λ dimension which are likely to be instrumental artefacts. In this paper we integrate the spectra into three bands to average out such errors.

However, there are concerns that the considerably lower values of S seen at some λ during the recent solar minimum, as shown in figure 2, are an instrumental effect: this is because these values all come from the one instrument (SIM on SORCE) and are inconsistent with previously successful models of UV irradiance [7]. To investigate this, we here also consider a change in both the instrument zero-level offset and its sensitivity (gain) between SIM and the previous instruments. We can do this because the SIM instrument was operated at the same time as SUSIM on UARS over the interval May 2003–July 2005. Because this was at a time when S was falling rapidly after the solar maximum, this overlap can be used to evaluate both the gain and offset of SIM compared to SUSIM, and hence the data composite. Figure 3 shows one such a comparison (this example is for a wavelength of $\lambda = 179$ nm). The blue curve in the left hand plot gives the monthly means of the SUSIM data, the red curve is the monthly means of the SIM data. The right hand panel in figure 3 is a scatter plot for the interval where these sequences overlap: the correlation coefficient is very high ($r = 0.93$) but the slope of the regression is not unity, implying SIM may indeed have a different gain factor than SUSIM. Using the best-fit least-squares ordinary regression, the SIM data can be made consistent with the SUSIM data, giving the green curve in the left hand plot. It can be seen that the recent solar minimum is not as deep for the re-calibrated green curve as it was for the uncalibrated red curve (but note that for this λ it is still slightly deeper than for the previous minimum seen in the SUSIM data). For some λ this calibration makes the recent minimum even deeper, but most cases are as in figure 3.

Parts (a)–(c) of figure 4 show the variations of monthly means of the average S over λ bands of 120–200 nm, 200–270 nm and 270–400 nm (referred to here as S_{FUV}, S_{MUV} and S_{NUV}, respectively). Consider first the black curves, which are taken from figure 2 directly—i.e. the irradiance data have been corrected only for zero-level offset changes (using the procedure demonstrated by figure 1). Figure 4(a) shows that the three minima in S_{FUV} show a consistent but very slight decline, whereas S_{MUV} shows a slight decline between the first two and then a much lower value in the third (figure 4(b)). A smaller drop (relative to the solar cycle amplitude) is seen for the only two minima in the useable S_{NUV} data (figure 4(c)). On the other hand, if we first adjust the SIM data for each wavelength using the linear regressions of the type shown in figure 3 (i.e., we correct for both instrument gain change and zero-level offset at this particular data join) we obtain the mauve lines (which prior to the start of the SIM data are identical the black line). In all three bands the composite data now show a slight decline from one minimum to the next, but the third minimum is less deep than for the black line in all three cases (considerably so for S_{MUV}).

Over the same interval as covered by these S_{FUV}, S_{MUV} and S_{NUV} composite sequences, the solar-minimum Total Solar Irradiance (TSI, absolute values of which are dominated by the visible and near IR emissions but the solar cycle variation of which is dominated by the UV [34, 35]) has been reported to have fallen to slightly lower values [1, 36], suggesting a slight long-term trend mirroring that in F_S, the open solar flux [37–39] and consistent with reconstructions of the TSI variation over past centuries [40, 41]. The inferred long-term variations in $F10.7$, the open solar flux F_S, and the related galactic cosmic ray (GCR) fluxes are shown in figure 5. In figure 5(a), monthly means of $F10.7$ are shown in mauve

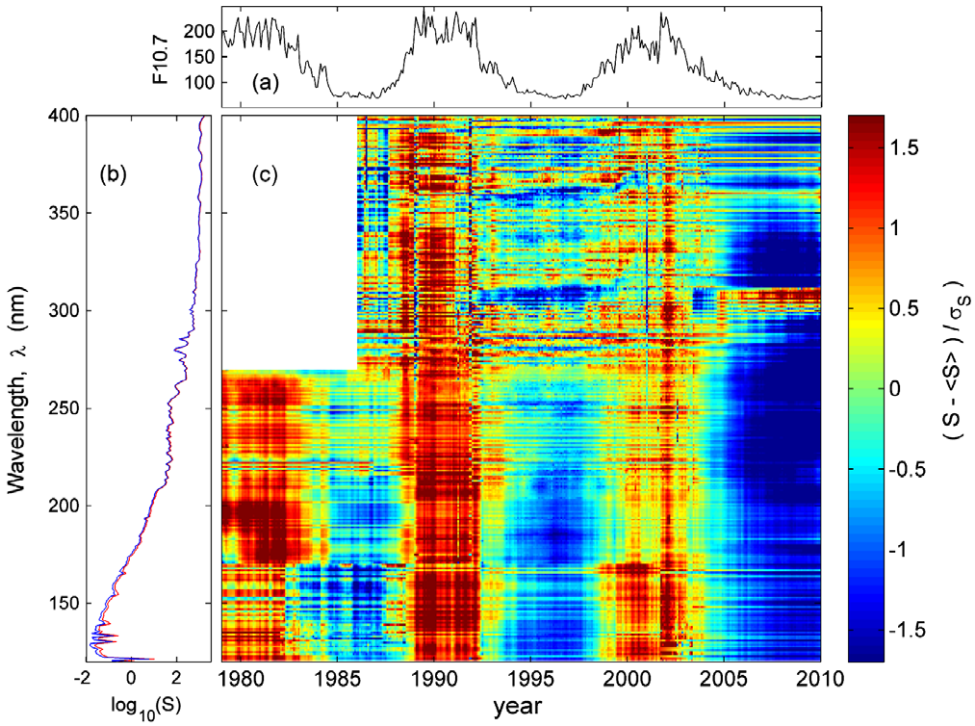

Figure 2. (a) Temporal variation of $F10.7$. (b) Solar UV spectrum: the maximum and minimum of the monthly spectral irradiance S are shown (in red and blue, respectively) as a function of wavelength, λ. (c) Normalized variations in S, $(S - \langle S \rangle)/\sigma_S$ where $\langle S \rangle$ and σ_S are the full data set means and standard deviations of S at that λ, as a function of time t and λ. SORCE data are used after 1 May 2004.

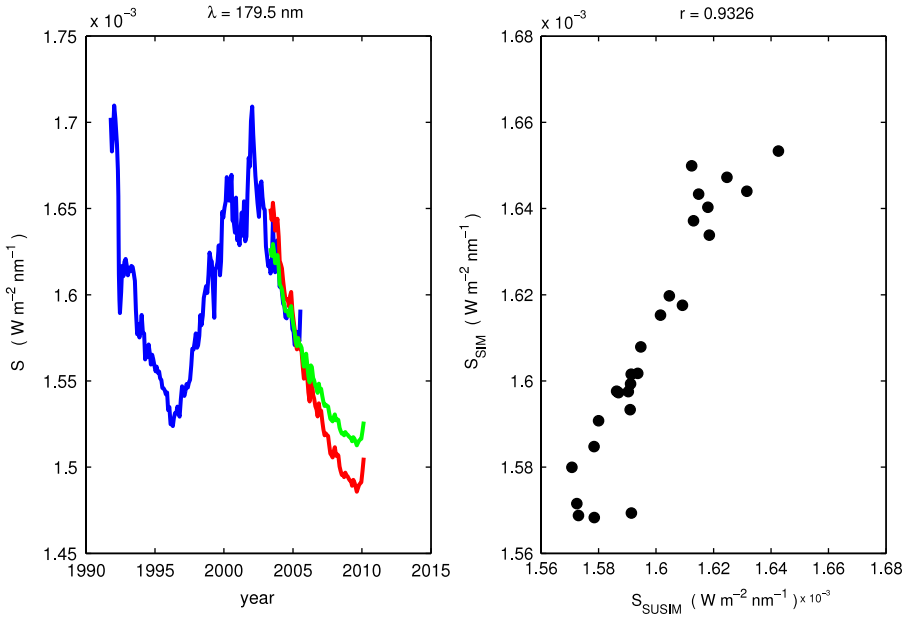

Figure 3. Illustration of the procedure used to calibrate the SORCE SIM instrument. (left). The blue, red and green lines show monthly means of, respectively, the UARS SUSIM data, the SORCE SIM data and the re-calibrated SORCE SIM data (using the regression shown in the right hand panel). (right). Scatter plot of the overlapping SUSIM and SIM monthly means for May 2003–July 2005. This example is for wavelength $\lambda = 179.5$ nm and the correlation coefficient for the scatter plot is $r = 0.93$.

and the black line shows an extrapolation using the highly correlated observations of sunspot numbers, R (correlation coefficient in annual means $r = 0.96$). The Ca-II lines are attenuated in the atmosphere but, unlike the Mg-II lines, can be observed from the ground: historic measurements have been reported as showing a variation that very closely matches that shown in figure 5(a) [42]; however, there is debate about the calibration of these data [31, 43]. Figure 5(b) shows (in orange) the Antarctic McMurdo neutron monitor counts M, here scaled in terms of heliospheric cosmic ray modulation parameter, Φ [44], using a linear regression of monthly values (correlation coefficient $r = -0.96$). The

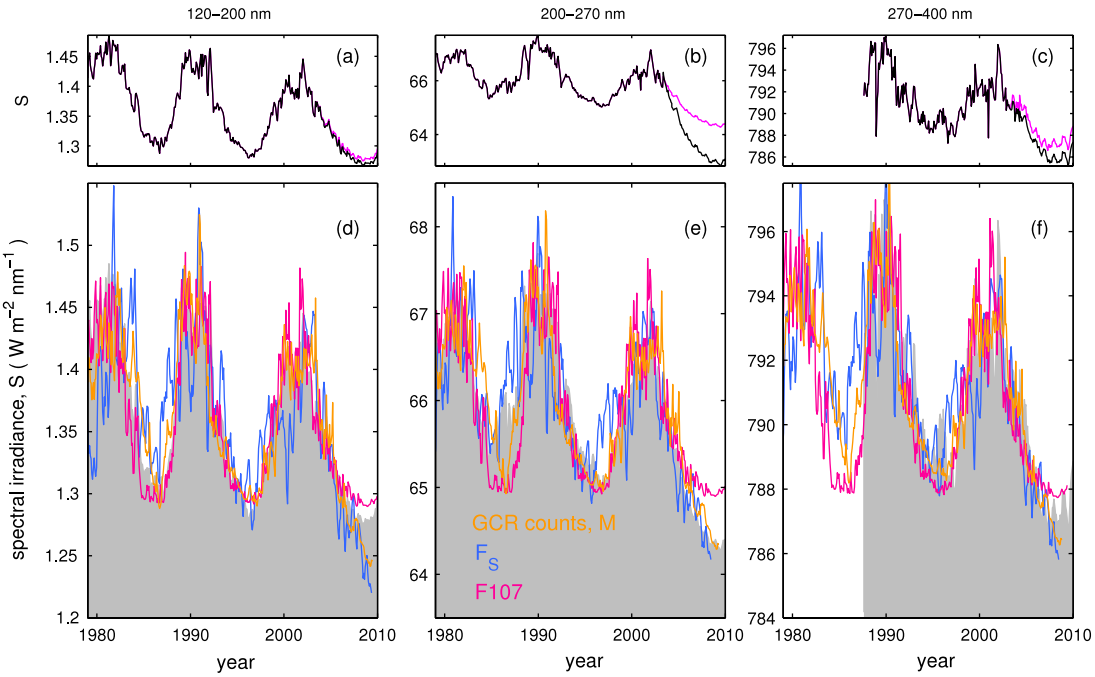

Figure 4. Variations of mean UV spectral irradiance in 3 wavelength bands: FUV, 120–200 nm (left); MUV, 200–270 nm (centre) and NUV, 270–400 nm (right) (respectively, $S_{\rm FUV}$, $S_{\rm MUV}$, and $S_{\rm NUV}$): the monthly means shown in the top panels in black are composites using only zero-level offset corrections to the raw data (as illustrated by figure 1), whereas those shown in mauve use an additional gain calibration for the SORCE SIM instrument (as illustrated by figure 3). The mauve curves are also shown by the grey filled areas in the lower panels. The lower panels also show the best least-squares linear regression fits of the McMurdo neutron monitor GCR counts, M (in orange); the open solar flux $F_{\rm S}$ (in blue) and $F10.7$ (in mauve). Correlation coefficients, r (with significance levels in parentheses) with $F10.7$, $F_{\rm S}$ and M respectively, for $S_{\rm FUV}$ are 0.95 (99.9%), 0.71 (87.4%) and −0.89 (94.4%); for $S_{\rm MUV}$ are 0.81 (92.9%), 0.80 (92.2%) and −0.89 (94.2%); and for $S_{\rm NUV}$ are 0.82 (99.6%), 0.83 (89.8%) and −0.87 (99.7%).

black line in figure 5(b) is the reconstruction of annual means of Φ by Usoskin *et al* [45]. Figure 5(c) shows the open solar flux, $F_{\rm S}$: blue values are 27 day (solar rotation) means from interplanetary magnetic field observations [37] and the black line shows annual means derived from geomagnetic activity indices [38, 39]. There is a major difference between the variations shown in figure 5 in that $F10.7$ (and Ca-II) show repeated returns to almost the same level at each solar minimum whereas the heliospheric indices $F_{\rm S}$ and Φ (and hence cosmic ray fluxes and cosmogenic isotope abundances) show centennial drift between solar minima.

The lower panels of figure 4 show the best ordinary linear regression fits of monthly means of $F10.7$, $F_{\rm S}$, and cosmic ray fluxes (we here use the McMurdo count rate M shown in orange in figure 5(b)) to the $S_{\rm FUV}$, $S_{\rm MUV}$ and $S_{\rm NUV}$ composites. We include the gain correction to the SIM data. The legend gives the correlation coefficients r and their significance levels. The good agreement on short timescales means that r for $F10.7$ is high in all 3 bands but the inferred long-term trends in $S_{\rm MUV}$ and $S_{\rm NUV}$ are better fitted by M and $F_{\rm S}$. Note that correlations for $F_{\rm S}$ are consistently lower because the data sequence is much noisier on these monthly timescales.

Chromospheric UV emission is closely linked to the local magnetic field [46] rather than that at the top of the solar corona (i.e., the open solar flux, $F_{\rm S}$). Because inward and outward magnetic field within pixels cancel, solar magnetographs reveal logarithmically greater field strengths (in the photosphere, just below the chromosphere) as resolution is increased [47, 48]. Much of this 'hidden' magnetic field seems not to show a solar cycle dependence, and so that part is thought to arise from turbulent motions in the quiet Sun: however, a second component implies an additional cascade down in scale sizes from the larger flux tubes emerging in sunspot groups [49, 50]. We note that the extent to which this hidden flux influences UV emissions also remains controversial; however, the time constant for this cascade appears to be of order 1–2 yrs which, coincidentally, is similar to the larger of two time constants for the magnetic flux in sunspot groups to evolve into $F_{\rm S}$ [51]. This offers one potential explanation of why heliospheric indices such as $F_{\rm S}$, Φ, M and cosmogenic isotopes might be useful proxies for UV emission even though they relate to the solar magnetic field in a quite different locations (respectively, the top and base of the solar atmosphere): a correlation could arise because both UV emission and open solar flux would be enhanced by increases in sunspot activity but they decay away with similar time constants.

3. Atmospheric response

The indication that key ozone-producing and heating wavelengths in the MUV may show long-term trends, similar to those in heliospheric proxies such as $F_{\rm S}$, M and Φ, depends critically on the intercalibration of the various radiometric records which remains highly uncertain. In this section, we take a different approach and search for the effects in Earth's

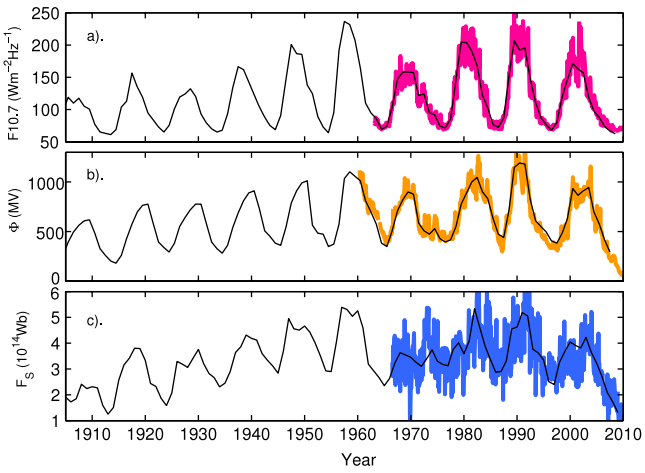

Figure 5. Variations of solar parameters. Coloured lines show monthly or 27 day means, black lines are annual means for extended data sequences. (a) The $F10.7$ index (monthly values in mauve), extrapolated using the highly correlated observations of sunspot numbers, R (correlation coefficient in annual means $r = 0.96$); (b) the Antarctic McMurdo neutron monitor counts M scaled in terms of heliospheric modulation parameter [44] Φ (from a linear regression of monthly values, in orange, with correlation coefficient $r = -0.96$): the black line gives the annual mean Φ reconstruction of Usoskin *et al* [45]. (c) The open solar flux, F_S: blue values are 27 day (solar rotation) means from IMF observations [37] the black line shows annual means derived from geomagnetic activity indices [38, 39].

atmosphere. We use the European Centre for Medium-Range Weather Forecasting (ECMWF) re-analysis dataset for 1979–2002, updated to 2008 using ECMWF operational analysis. A standard multiple linear regression is performed on annual means to separate the atmospheric dataset into contributions from various climate indices. This analysis is exactly as used in the papers by Crook and Gray [52] and Frame and Gray [53] and the reader is referred to these papers for full details. We employ a constant term, a linear trend, a stratospheric optical depth index, a multivariate ENSO index, two orthogonal quasi-biennial oscillation indices, and a solar variability proxy (one of $F10.7$, F_S, TSI, Φ and M). The results are shown in figure 6 for zonal means of temperature T (top) and of zonal wind U (bottom). Results for TSI (not shown) are quite similar in form, but weaker in amplitude, to those for $F10.7$. The solar effect on equatorial lower stratospheric temperatures (previously found using $F10.7$ [11, 52, 53]) can be seen in figure 6(a) and peaks at $k/\sigma = 0.3$ K σ^{-1}, where k is the regression slope and σ is the standard deviation of the solar parameter. (Note that normalizing k by σ allows for the different units and ranges of the various solar indices so that we can compare the amplitudes of the responses). Figures 6(b) and (c) show stronger effects peaking at 0.5 K σ^{-1} for M and F_S (with greater significance and over a larger region). Modelling [9] and data analysis [10] has indicated that the solar effect on T in the lower equatorial stratosphere can influence the jet streams in the underlying troposphere. This can be seen in figure 6(d) (for $F10.7$) where the effect on U in the mid-latitude troposphere peaks at about $k/\sigma = -0.3$ m s$^{-1}\sigma^{-1}$. However, the effect is considerably stronger for F_S (k/σ peaking at -0.8 m s$^{-1}\sigma^{-1}$ in figure 6(f)) and the statistical significance is greater and over a wider region. The additional response for F_S (figure 6(f)) is mainly in the northern hemisphere, being somewhat more asymmetric than that for M (figure 6(e)). Figure 6(c) also shows a small band of significant surface temperature response at middle northern latitudes where recent studies have revealed solar signatures in regional climate, particularly in the European sector [24–26].

We have checked that the larger responses seen in figure 6 for F_S and M do not arise from an interplay with the linear trend. Plots equivalent to figure 6 for the best-fit trend term using all three solar indices are virtually identical. (We do not reproduce those plots here as the trend magnitudes are not thought to be reliable because of the way the ERA re-analysis dataset is constructed.) For the analysis using $F10.7$, Frame and Gray [53] investigated how the percentage variances were apportioned between the different terms and the errors introduced (e.g., by small changes in the data period employed) and their results are not significantly changed by the use of the other solar indices. Also, the regression analysis included an AR3 autoregressive noise model [53] and the residual was checked to ensure it is acceptably small, (i.e., that the residual is random noise and there is no significant remaining unexplained variations).

4. Discussion and conclusions

The work presented here is consistent with the interpretation of a recently reported effect [25] of solar variability on the North Atlantic Oscillation (NAO) and European winter temperatures over the interval 1659–2010 in terms of top-down modulation of the blocking phenomenon [52, 53]. In fact, Woollings *et al* [26] show that the solar response pattern is, despite being similar in form to that of the NAO, significantly different in that it reaches further east. These authors also show that open solar flux has a much stronger control over blocking events in this sector than the previously reported effect of $F10.7$ [55].

There is seasonality in the solar responses reported here. This is expected as modulation of upwards-propagating planetary waves in wintertime, and the associated stratosphere–troposphere interaction, is most widely believed to be the key mechanism [8, 11]. In addition, the tropospheric signature is a response of the eddy-driven jet streams, and these are at their strongest and most responsive in winter. While the results are presented here as annual means, the regression analysis was actually carried out on monthly mean data and thus takes this seasonality into account. The seasonal evolution of the $F10.7$ cm flux regression was described in detail by Frame and Gray [53] and this was not significantly affected by using either the open solar flux F_S nor the cosmic ray flux, M, instead of $F10.7$.

The relationship between the open solar flux F_S and UV spectral irradiance changes inferred here provides an explanation of why the open solar flux was a valuable proxy for solar activity in the recent studies by Lockwood *et al* [25] and Woollings *et al* [26]. In addition, F_S is correlated with other parameters such as the level of geomagnetic activity and solar wind dynamic pressure and a relationship with UV variability

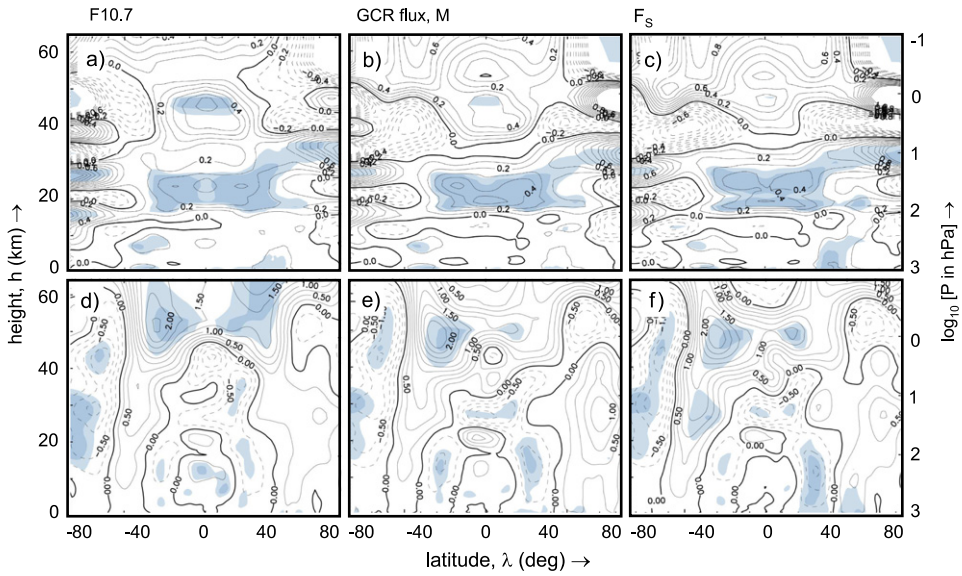

Figure 6. Results of multiple regression analyses using different solar parameters for (top) zonal mean temperature T and (bottom) zonal mean zonal wind, U. (a) and (d) are for $F10.7$; (b) and (e) are for the McMurdo GCR flux, M and (c) and (f) are for the open solar flux, F_S. Contours show k/σ (where k is the regression coefficient and σ is the standard deviation of the solar parameter) as a function of height h and latitude λ (contours are labelled in units of K σ^{-1} in the upper panels and m s^{-1} σ^{-1} in the lower ones). The light and dark grey areas show where the significance from Student's t-test exceeds 95% and 99%, respectively.

may be responsible for persistent reports of a relationship between these phenomena and the NAO [56–59]. This is a much more satisfactory explanation than any causal link, for which the unexplained amplification required would be massive (the energy density of the solar wind being smaller than the TSI by a factor of order 10^5 and the currents that it generates, and that cause geomagnetic activity and heating, are in the upper atmosphere where the mass is of order 10^{-3} of the total atmospheric mass).

Furthermore, F_S is highly anticorrelated with cosmic ray fluxes reaching Earth on a wide range of timescales [60]. This makes any relationship of F_S with UV emissions and top-down solar forcing a relevant factor in the considerable debate about reported correlations between climate (in particular global or regional cloud cover) and GCRs. Indeed some authors have noted that apparent solar cycle variations in cloud cover are in better agreement with the UV irradiance variation than that of GCRs [61–63], although we note that other studies that have tried to discriminate between electromagnetic irradiance and direct cosmic ray effects do find some evidence for the latter [64, 65]. A great many palaeoclimate studies have found links between regional or local climate indicators and cosmogenic isotopes and so it has been argued that this is either evidence for a direct cosmic ray effect or that the cosmic rays are proxy indicators for the correlated irradiance variability [66]. In particular, the much cited and much debated paper by Bond *et al* [67] revealed a persistent correlation during the Holocene between ice-rafted debris in the North Atlantic region and cosmogenic isotopes. The results presented here and in the recent paper by Woollings *et al* [26] suggest that solar UV variability and top-down solar forcing can introduce regional changes in the troposphere in the region studied by Bond *et al* and that these may vary on centennial timescales, as recently reported in the Central England temperature records by Lockwood *et al* [25]. The implication is that seasonal/regional evaluation of past and future climate change will be improved by models with adequate resolution in the stratosphere to reproduce top-down solar forcing.

Acknowledgments

We thank: the SORCE/SIM team and LASP, Colorado for the UV spectral data; the Bartol Research Institute, University of Delaware, for the McMurdo neutron monitor data, Matthew DeLand and Richard Cebula for their UV data composite; Ilya Usoskin for the modulation parameter data and ECMWF for the atmospheric re-analysis data. The interplanetary and geomagnetic data were obtained via the WDC for Solar Terrestrial Physics, Chilton, UK. We thank the many scientists who contributed to all these datasets and others for valuable discussions.

References

[1] Lockwood M 2010 Solar change and climate: an update in the light of the current exceptional solar minimum *Proc. R. Soc.* A **466** 303–29

[2] Harder J W, Fontenla J M, Pilewskie P, Richard E C and Woods T N 2009 Trends in solar spectral irradiance variability in the visible and infrared *Geophys. Res. Lett.* **36** L07801

[3] Lean J 2000 Evolution of the Sun's spectral irradiance since the Maunder minimum *Geophys. Res. Lett.* **27** 2425–8

[4] DeLand M T and Cebula R P 2008 Creation of a composite solar ultraviolet irradiance data set *J. Geophys. Res.* **113** A11103

[5] Haigh J D, Winning A R, Toumi R and Harder J W 2010 An influence of solar spectral variations on radiative forcing of climate *Nature* at press

[6] Gray L J *et al* 2010 Solar influences on climate *Rev. Geophys.* at press (doi:10.1029/2009RG000282)

[7] Lean J L 2010 How bright is the sun? How does it vary? Why do we care? *B.A.M.S.* at press

[8] Matthes K, Kuroda Y, Kodera K and Langematz U 2006 Transfer of the solar signal from the stratosphere to the troposphere: northern winter *J. Geophys. Res.* **111** D06108

[9] Haigh J D 1996 The impact of solar variability on climate *Science* **272** 981–4

[10] Haigh J D 2003 The effects of solar variability on the Earth's climate *Phil. Trans. R. Soc.* A **361** 95–111

[11] Gray L J, Crooks S, Pascoe C, Sparrow S and Palmer M 2004 Solar and QBO influences on the timing of stratospheric sudden warmings *J. Atmos. Sci.* **61** 2777–96

[12] Baldwin M P and Dunkerton T J 1999 Propagation of the Arctic oscillation from the stratosphere to the troposphere *J. Geophys. Res.* **104** 30,937–40,946

[13] Plumb R A and Semeniuk K 2003 Downward propagation of extra-tropical zonal wind anomalies *J. Geophys. Res.* **108(D7)** 4223

[14] Kushner P J and Polvani L M 2004 Stratosphere–troposphere coupling in a relatively simple AGCM: the role of eddies *J. Clim.* **17** 629–39

[15] Simpson I R, Blackburn M and Haigh J D 2009 The role of eddies in driving the tropospheric response to stratospheric heating perturbations *J. Atmos. Sci.* **66** 1347–65

[16] Shindell D T, Schmidt G A, Miller R L and Rind D 2001 Northern Hemisphere winter climate response to greenhouse gas, ozone, solar, and volcanic forcing *J. Geophys. Res.* **106** 7193–210

[17] Perlwitz J and Harnik N 2003 Observational evidence of a stratospheric influence on the troposphere by planetary wave reflection *J. Clim.* **16** 3011–26

[18] Scaife A A, Knight J R, Vallis G K and Folland C K 2005 A stratospheric influence on the winter NAO and North Atlantic surface climate *Geophys. Res. Lett.* **32** L18715

[19] Thompson D W J, Baldwin M P and Solomon S 2005 Stratosphere–troposphere coupling in the Southern Hemisphere *J. Atmos. Sci.* **62** 708–15

[20] Meehl G A, Arblaster J M, Branstator G and van Loon H 2008 A coupled air–sea response mechanism to solar forcing in the Pacific region *J. Clim.* **21** 2883–97

[21] Rind D, Lean J, Lerner J, Lonergan P and Leboissitier A 2008 Exploring the stratospheric/tropospheric response to solar forcing *J. Geophys. Res.* **113** D24103

[22] Meehl G A, Arblaster J M, Sassi F, Matthes K and van Loon H 2009 Amplifying the Pacific climate system response to a small 11 year solar cycle forcing *Science* **325** 1114–8

[23] Stott P A, Jones G S and Mitchell J F B 2003 Do models underestimate the solar contribution to recent climate change? *J. Clim.* **16** 4079–93

[24] Lean J L and Rind D H 2008 How natural and anthropogenic influences alter global and regional surface temperatures: 1889–2006 *Geophys. Res. Lett.* **35** L18701

[25] Lockwood M, Harrison R G, Woollings T and Solanki S K 2010 Are cold winters in the UK associated with low solar activity? *Environ. Res. Lett.* **5** 024001

[26] Woollings T, Lockwood M, Masato G, Bell C and Gray L 2010 Enhanced signature of solar variability in Eurasian winter climate *Geophys. Res. Lett.* at press (doi:10.1029/2010GL044601)

[27] Camp C D and Tung K K 2007 Surface warming by the solar cycle as revealed by the composite mean difference projection *Geophys. Res. Lett.* **34** L14703

[28] Gleisner H, Thejll P, Stendel M, Kaas E and Machenhauer B 2005 Solar signals in tropospheric re-analysis data: comparing NCEP/NCAR and ERA40 *J. Atmos. Sol.-Terr. Phys.* **67** 785–91

[29] Gleisner H and Thejll P 2003 Patterns of tropospheric response to solar variability *Geophys. Res. Lett.* **30** 17129

[30] Floyd L, Tobiska W K and Cebula R P 2002 Solar UV irradiance, its variation, and its relevance to the earth *Adv. Space Res.* **29** 1427–40

[31] Ermolli I, Solanki S K, Tlatov A G, Krivova N A, Ulrich R K and Singh J 2009 Comparison among Ca II K spectroheliogram time series with an application to solar activity studies *Astrophys. J.* **698** 1000–9

[32] Viereck R A, Floyd L E, Crane P C, Woods T N, Knapp B G, Rottman G, Weber M, Puga L C and DeLand M T 2004 A composite Mg II index spanning from 1978 to 2003 *Space Weather* **2** S10005

[33] Dudok de Wit T, Kretzschmar M, Lilensten J and Woods T 2009 Finding the best proxies for the solar UV irradiance *Geophys. Res. Lett.* **36** L10107

[34] Krivova N A, Solanki S K and Floyd L 2006 Reconstruction of solar 495 UV irradiance in cycle 23 *Astron. Astrophys.* **452** 631–9

[35] Krivova N A, Solanki S K, Wenzler T and Podlipnik B 2009 Reconstruction of solar UV irradiance since 1974 *J. Geophys. Res.* **114** D00I04

[36] Fröhlich C 2009 Evidence of a long-term trend in total solar irradiance *Astron. Astrophys.* **501** L27–30

[37] Lockwood M, Stamper R and Wild M N 1999 A doubling of the sun's coronal magnetic field during the last 100 years *Nature* **399** 437–9

[38] Lockwood M, Owens M and Rouillard A P 2009 Excess open solar magnetic flux from satellite data: II. A survey of kinematic effects *J. Geophys. Res.* **114** A11104

[39] Lockwood M, Rouillard A P and Finch I D 2009 The rise and fall of open solar flux during the current grand solar maximum *Astrophys. J.* **700** 937–44

[40] Krivova N A, Balmaceda L and Solanki S K 2007 Reconstruction of solar total irradiance since 1700 from the surface magnetic flux *Astron. Astrophys.* **467** 335–46

[41] Steinhilber F, Beer J and Fröhlich C 2009 Total solar irradiance during the Holocene *Geophys. Res. Lett.* **36** L19704

[42] Foukal P, Bertello L, Livingston W C, Pevtsov A P, Singh J T, Tlatov A G and Ulrich R K 2009 A century of solar Ca II measurements and their implication for solar UV driving of climate *Sol. Phys.* **255** 229–38

[43] Tlatov A G, Pevtsov A A and Singh J A 2009 New method of calibration of photographic plates from three historic data sets *Sol. Phys.* **255** 239–51

[44] Usoskin I G, Alanko-Huotari K, Kovaltsov G A and Mursula K 2005 Heliospheric modulation of cosmic rays: monthly reconstruction for 1951–2004 *J. Geophys. Res.* **110** A12108

[45] Usoskin I G, Mursula K, Solanki S K, Schüssler M and Kovaltsov G A 2002 A physical reconstruction of cosmic ray intensity since 1610 *J. Geophys. Res.* **107(A11)** 1374

[46] Louitcheva M, Solanki S K and White S W 2009 The relationship between chromospheric emissions and magnetic field strength *Astron. Astrophys.* **497** 273–85

[47] Bueno T J, Shchukina N and Ramos A A 2004 A substantial amount of hidden magnetic energy in the quiet Sun *Nature* **430** 326–9

[48] Almeida J S 2009 The dynamic magnetic quiet Sun: physical mechanisms and UV signature *Astrophys. Space Sci.* **320** 121–7

[49] Pauluhn A and Solanki S K 2003 Dependence of UV radiance of the quiet Sun on the solar cycle: surface magnetic fields as the cause *Astron. Astrophys.* **407** 359–67

[50] Chapman G A and Hoffer A S 2006 The growth of facular area surrounding large, decaying sunspots *Sol. Phys.* **237** 321–8

[51] Vieira L E A and Solanki S K 2010 Evolution of the solar magnetic flux on timescales of years to millennia *Astron. Astrophys.* **509** A100

[52] Frame T and Gray L J 2010 The 11-year solar cycle in ERA-40 data: an update to 2008 *J. Clim.* **23** 2213–22

[53] Crook S A and Gray L J 2005 Characterization of the 11-year solar signal using a multiple regression analysis of the ERA-40 dataset *J. Clim.* **18** 996–1014

[54] Woollings T, Charlton-Perez A, Ineson S, Marshall A G and Masato G 2010 Associations between stratospheric variability and tropospheric blocking *J. Geophys. Res.* **115** D06108

[55] Barriopedro D, García-Herrera R and Huth R 2008 Solar modulation of Northern Hemisphere winter blocking *J. Geophys. Res.* **113** D14118

[56] Boberg F and Lundstedt H 2002 Solar wind variations related to fluctuations of the North Atlantic Oscillation *Geophys. Res. Lett.* **29** 1718

[57] Lu H, Jarvis M J and Hibbins R E 2008 Possible solar wind effect on the northern annular mode and northern hemispheric circulation during winter and spring *J. Geophys. Res.* **113** D23104

[58] Bochníček J and Hejda P 2005 The winter NAO pattern changes in association with solar and geomagnetic activity *J. Atmos. Sol.-Terr. Phys.* **67** 17–32

[59] Thejll P, Christiansen B and Gleisner H 2003 On correlations between the North Atlantic Oscillation, geopotential heights and geomagnetic activity *Geophys. Res. Lett.* **30** 1347

[60] Rouillard A P and Lockwood M 2004 Oscillations in the open solar magnetic flux with period 1.68 years: imprint on galactic cosmic rays and implications for heliospheric shielding *Ann. Geophys.* **22** 4381–4396

[61] de Jager C and Usoskin I 2006 On possible drivers of Sun-induced climate changes *J. Atmos. Sol.-Terr. Phys.* **68** 2053–60

[62] Erlykin A D, Sloan T and Wolfendale A W 2010 Correlations of clouds, cosmic rays and solar irradiation over the Earth *J. Atmos. Sol.-Terr. Phys.* **72** 151–6

[63] Udelhofen P M and Cess R D 2001 Cloud cover variations over the united states: an influence of cosmic rays or solar variability? *Geophys. Res. Lett.* **28** 2617–20

[64] Voiculescu M, Usoskin I G and Mursula K 2006 Different response of clouds to solar input *Geophys. Res. Lett.* **33** L21802

[65] Harrison R G 2008 Discrimination between cosmic ray and solar irradiance effects on clouds, and evidence for geophysical modulation of cloud thickness *Proc. R. Soc.* A **464** 2575–90

[66] Lockwood M 2006 What do cosmogenic isotopes tell us about past solar forcing of climate? *Space Sci. Rev.* **125** 95–109

[67] Bond G, Kromer B, Beer J, Muscheler R, Evans M N, Showers W, Hoffman S, Lotti-Bond R, Hajdas I and Bonani G 2001 Persistent solar influence on North Atlantic climate during the Holocene *Science* **294** 2130–6